



ACADEMIC  
PRESS

Available online at [www.sciencedirect.com](http://www.sciencedirect.com)

SCIENCE @ DIRECT®

Journal of Solid State Chemistry 174 (2003) 221–228

JOURNAL OF  
SOLID STATE  
CHEMISTRY

<http://elsevier.com/locate/jssc>

# High-temperature synthesis, single-crystal X-ray structure determination and solid-state NMR investigations of $\text{Ba}_7[\text{SiO}_4][\text{BO}_3]_3\text{CN}$ and $\text{Sr}_7[\text{SiO}_4][\text{BO}_3]_3\text{CN}$

Sabine Schmid, Jürgen Senker, and Wolfgang Schnick\*

Department Chemie, Ludwig-Maximilians-Universität, Butenandtstraße 5-13 (Haus D), D-81377 München, Germany

Received 24 December 2002; received in revised form 16 April 2003; accepted 25 April 2003

## Abstract

The novel alkaline earth silicate borate cyanides  $\text{Ba}_7[\text{SiO}_4][\text{BO}_3]_3\text{CN}$  and  $\text{Sr}_7[\text{SiO}_4][\text{BO}_3]_3\text{CN}$  have been obtained by the reaction of the respective alkaline earth metals  $M = \text{Sr}, \text{Ba}$ , the carbonates  $M^{\text{II}}\text{CO}_3$ , BN, and  $\text{SiO}_2$  using a radiofrequency furnace at a maximum reaction temperature of 1350°C and 1450°C, respectively. The crystal structures of the isotypic compounds  $M^{\text{II}}_7[\text{SiO}_4][\text{BO}_3]_3\text{CN}$  have been determined by single-crystal X-ray crystallography ( $P6_3mc$  (no. 186),  $Z = 2$ ,  $a = 1129.9(1)$  pm,  $c = 733.4(2)$  pm,  $R_1 = 0.0336$ ,  $wR_2 = 0.0743$  for  $M^{\text{II}} = \text{Ba}$  and  $a = 1081.3(1)$  pm,  $c = 695.2(1)$  pm,  $R_1 = 0.0457$ ,  $wR_2 = 0.0838$  for  $M^{\text{II}} = \text{Sr}$ ). Both ionic compounds represent a new structure type, and they are the first examples of silicate borate cyanides. The cyanide ions are disordered and they are surrounded by  $\text{Ba}^{2+}/\text{Sr}^{2+}$  octahedra, respectively. These octahedra share common faces building chains along [001]. The  $[\text{BO}_3]^{3-}$  ions are arranged around these chains. The  $[\text{SiO}_4]^{4-}$  units are surrounded by  $\text{Ba}^{2+}/\text{Sr}^{2+}$  tetrahedra, respectively. The title compounds additionally have been investigated by  $^{11}\text{B}$ ,  $^{13}\text{C}$ ,  $^{29}\text{Si}$ , and  $^1\text{H}$  MAS-NMR as well as IR and Raman spectroscopy confirming the presence of  $[\text{SiO}_4]^{4-}$ ,  $[\text{BO}_3]^{3-}$ , and  $\text{CN}^-$  ions.

© 2003 Elsevier Science (USA). All rights reserved.

**Keywords:** Borates; Silicates; Cyanides; Crystal structure

## 1. Introduction

During the last few years we developed and refined a synthetic approach for novel oligonary nitrides and oxonitrides of silicon and aluminum [1], and in the meantime we have also extended our investigations on nitridoborates [2]. Recently, we succeeded to synthesize the first oxonitridoborate, namely  $\text{Sr}_3[\text{B}_3\text{O}_3\text{N}_3]$  [3]. This compound was obtained by the reaction of  $\text{SrCO}_3$  and poly(boron amide imide). In order to synthesize the isotypic compound with barium instead of strontium we utilized  $\text{BaCO}_3$ , BN, and additionally metallic Ba as starting materials. Surprisingly, the reaction product was neither  $\text{Ba}_3[\text{B}_3\text{O}_3\text{N}_3]$  nor another oxonitride. By serendipity we obtained the title compound  $\text{Ba}_7[\text{SiO}_4][\text{BO}_3]_3\text{CN}$ , which must have been formed by a complex redox reaction under involvement of a silica contamination in the crucible. Subsequently we succeeded to directly synthesize single-phase  $\text{Ba}_7[\text{SiO}_4][\text{BO}_3]_3\text{CN}$  by

the reaction of Ba, BN,  $\text{BaCO}_3$  and  $\text{SiO}_2$ . Isotypic  $\text{Sr}_7[\text{SiO}_4][\text{BO}_3]_3\text{CN}$  analogously was obtained utilizing Sr and  $\text{SrCO}_3$  instead.

## 2. Experimental procedure

For the high-temperature synthesis of  $\text{Ba}_7[\text{SiO}_4][\text{BO}_3]_3\text{CN}$  and  $\text{Sr}_7[\text{SiO}_4][\text{BO}_3]_3\text{CN}$  we have used a radiofrequency (rf) furnace. Details of the experimental setup are given in Ref. [4]. As starting materials for the preparation we have used BN [5],  $\text{SiO}_2$  (Fluka, purity  $\geq 99\%$ ),  $\text{BaCO}_3$  (Grüssing, 99%),  $\text{SrCO}_3$  (Alfa Aesar, purity 99.9%), metallic barium (ABCR, purity 99.9%) and metallic strontium (ABCR, purity 99.95%), respectively.

### 2.1. Synthesis of $\text{Ba}_7[\text{SiO}_4][\text{BO}_3]_3\text{CN}$

$\text{Ba}_7[\text{SiO}_4][\text{BO}_3]_3\text{CN}$  has been obtained by high-temperature reaction of 396.5 mg (2.01 mmol)  $\text{BaCO}_3$ , 50.8 mg (2.05 mmol) BN, 38.8 mg (0.64 mmol)  $\text{SiO}_2$ ,

\*Corresponding author. Fax: +49-(0)2180-77440.

E-mail address: [wolfgang.schnick@uni-muenchen.de](mailto:wolfgang.schnick@uni-muenchen.de) (W. Schnick).

and 450.3 mg (3.28 mmol) Ba. Under an atmosphere of pure argon, the starting compounds were filled into a tungsten crucible which was positioned in the center of the induction coil of an rf furnace. The reaction was then performed under an atmosphere of pure nitrogen (purified by silica gel, potassium hydroxide, molecular sieve,  $P_4O_{10}$ , and a BTS catalyst). The reaction batch was heated up to 750°C with a rate of 12.5°C/min, this temperature was held for 30 min and then it was increased with 6.7°C/min to 1350°C. After 45 min the product was cooled with 0.3°C/min to 200°C. Subsequently, the mixture was quenched to room temperature.

$Sr_7[SiO_4][BO_3]_3CN$  has been obtained by high-temperature reaction of 293.7 mg (1.99 mmol)  $SrCO_3$ , 55.6 mg (2.24 mmol) BN, 38.8 mg (0.64 mmol)  $SiO_2$ , and 309.8 mg (3.54 mmol) Sr. The reaction conditions were similar to the ones we used for the synthesis of  $Ba_7[SiO_4][BO_3]_3CN$ . The reaction batch was heated up to 750°C with a rate of 25°C/min, held for 30 min and then increased with 11.7°C/min to 1450°C. After 30 min the product was again cooled with 0.35°C/min to 200°C. Subsequently, the mixture was quenched to room temperature.  $Ba_7[SiO_4][BO_3]_3CN$  was obtained as a coarsely crystalline yellowish solid and  $Sr_7[SiO_4][BO_3]_3CN$  as white needles. Both compounds are rather sensitive against hydrolysis.

X-ray powder diffraction measurements were performed to ensure the absence of starting materials in the sample. The purity was confirmed via solid-state NMR. The composition of  $Ba_7[SiO_4][BO_3]_3CN$  ( $M = 1255.85$  g/mol) has been analyzed by ICP AES resulting in 76.97 mass% Ba (calc. 76.55%), 2.51% B (2.58%) and 2.17% Si (2.24%) which is in reasonable agreement with the structure model derived from the X-ray single-crystal structure analysis. The presence of cyanide ions ( $CN^-$ ) in the reaction product was proven by chemical analysis, vibrational spectroscopy (IR and Raman), and solid-state NMR.

### 3. Crystal structure analysis

Single-crystal X-ray diffraction data of  $Ba_7[SiO_4][BO_3]_3CN$  were collected on a Stoe STADI4 four-circle diffractometer using  $MoK\alpha$  radiation and the diffraction data of  $Sr_7[SiO_4][BO_3]_3CN$  were collected with a Stoe IPDS diffractometer using  $MoK\alpha$  radiation as well. According to the observed extinction conditions of the hexagonal/trigonal lattice (only reflections  $hh2hl$  and  $00l$  with  $l = 2n$ ) the space groups  $P31c$ ,  $P3r1c$ ,  $P6_3mc$ ,  $P6_3/mmc$  and  $P62m$  were considered. The structure solution and refinement, however, were possible only with space group  $P6_3mc$  (no. 186). The crystal structures of  $Ba_7[SiO_4][BO_3]_3CN$  and  $Sr_7[SiO_4][BO_3]_3CN$  have been solved by direct methods (SHELXS [6]) using the

software package Wingx [7] and were refined with anisotropic displacement parameters using SHELXL [6] for all atoms except those of the  $CN^-$  group and the disordered oxygen atoms.

Due to structural disorder of the cyanide ions it was not possible to resolve the carbon and nitrogen atoms. We found two independent peaks in the difference map for carbon and nitrogen in a distance of about 120 pm. But already after one refinement cycle the C and N atoms were located at the same position. Therefore we implemented only one atomic site for the  $CN^-$  group representing its center of gravity, which was only isotropically refined. One oxygen atom of the  $[SiO_4]^{4-}$  group (O1) was located on a  $12d$  site with half occupancy leading to a structural disorder between two different orientations of the  $[SiO_4]^{4-}$  group (see Fig. 1). Both orientations of the  $[SiO_4]^{4-}$  group are transformed into each other by a slight rotation along the Si–O4 bond which is parallel [001]. In order to investigate the nature of this disorder low-temperature X-ray single-crystal diffraction was performed. Extrapolation of the tensor elements of the anisotropic displacement parameters against  $T = 0$  K resulted in significant residual disorder. Thus both the low-temperature diffraction data and the MAS-NMR investigations seem to rule out a dynamic disorder but they are consistent with a statistical structural disorder of the  $[SiO_4]^{4-}$  groups.

It is noteworthy that the anisotropic displacement factor for one of the oxygen atoms of the borate group (O3) is significant larger in the strontium compound than it is in the barium compound. One reason for that could be some kind of minor disordering. Accordingly the bond length B1–O3 is 141 pm and the O3–B1–O2 angle is 115.7°. Further details of the X-ray data collection and the relevant crystallographic data are summarized in Tables 1 and 2. In Table 3 selected interatomic distances and angles are listed.

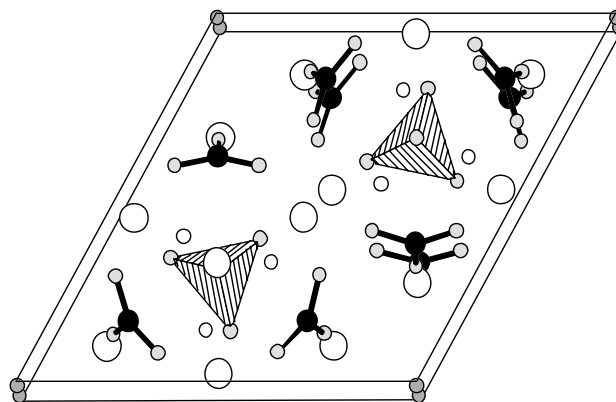


Fig. 1. Crystal structure of  $Ba_7[SiO_4][BO_3]_3CN$  (Ba white, B black, O light gray, CN medium gray, Si inside polyhedra), view along [001]. The split position of O1 is depicted as small white circles.

Table 1  
Crystallographic data of Ba<sub>7</sub>[SiO<sub>4</sub>][BO<sub>3</sub>]<sub>3</sub>CN and Sr<sub>7</sub>[SiO<sub>4</sub>][BO<sub>3</sub>]<sub>3</sub>CN at 293(2) K

Crystal Data		Ba <sub>7</sub> [SiO <sub>4</sub> ][BO <sub>3</sub> ] <sub>3</sub> CN	Sr <sub>7</sub> [SiO <sub>4</sub> ][BO <sub>3</sub> ] <sub>3</sub> CN
Formula		Ba <sub>7</sub> [SiO <sub>4</sub> ][BO <sub>3</sub> ] <sub>3</sub> CN	Sr <sub>7</sub> [SiO <sub>4</sub> ][BO <sub>3</sub> ] <sub>3</sub> CN
Crystal system, space group		Hexagonal, <i>P6<sub>3</sub>mc</i> (No. 186), <i>Z</i> = 2	
Unit cell dimensions		<i>a</i> = 1129.9(1) pm <i>c</i> = 733.4(2) pm	<i>a</i> = 1081.3(1) pm <i>c</i> = 695.2(1) pm
Cell volume		810.98(1) × 10 <sup>6</sup> pm <sup>3</sup>	706.3(1) × 10 <sup>6</sup> pm <sup>3</sup>
<i>F</i> (000)		1062	812
X-ray density $\rho$		5.086 g cm <sup>-3</sup>	4.212 g cm <sup>-3</sup>
Absorption coefficient		16.84 mm <sup>-1</sup>	26.38 mm <sup>-1</sup>
Habit		Yellow needle	White needle
Crystal size		0.479 × 0.123 × 0.111 mm <sup>3</sup>	0.25 × 0.07 × 0.05 mm <sup>3</sup>
<i>Data collection</i>			
Single-crystal X-ray diffractometer		Stoe STADI4	Stoe IPDS
Radiation			MoK $\alpha$ ( $\lambda$ = 71.073 pm)
Measured		Asymmetric unit and Friedel pairs	all octants
$2\theta_{\max}$		65°	56.14°
<i>h, k, l</i>		-17 ≤ <i>h</i> ≤ 17 -17 ≤ <i>k</i> ≤ 17 -11 ≤ <i>l</i> ≤ 11	-14 ≤ <i>h</i> ≤ 14 -13 ≤ <i>k</i> ≤ 14 -8 ≤ <i>l</i> ≤ 8
Measured reflections		4103	6040
Independent reflections		1109 ( <i>R</i> <sub>int</sub> = 0.0698)	603 ( <i>R</i> <sub>int</sub> = 0.0562)
Observed reflections ( <i>F</i> <sub>0</sub> <sup>2</sup> ≥ 4σ( <i>F</i> <sub>0</sub> <sup>2</sup> ))		988	496
Absorption correction		Numerical ( $\psi$ -scans)	Numerical (equivalents)
Used program			HABITUS [23]
Min./max. transmission		0.2226, 0.3201	0.0392, 0.0676
<i>Refinement</i>			
Program used for refinement			SHELXL-97 [6], refinement on <i>F</i> <sup>2</sup>
Refined parameters		51	51
Flack parameter		0.57157	0.45194
			Refined as inversion twin
Min./max. residual electron density		-1.40/1.75 e/Å <sup>3</sup>	-0.93/1.20 e/Å <sup>3</sup>
Extinction coefficient		0.001223	0.0
Weighting scheme ( <i>x/y</i> )		0.025200/4.1483	0.042100/3.7928
			$w^{-1} = \sigma^2 F_0^2 + (xP)^2 + yP$ ; $P = (F_0^2 + 2 F_c^2)/3$
Goodness-of-fit		1.132	1.077
<i>R</i> indices (all data)		<i>R</i> <sub>1</sub> = 0.0332 <i>wR</i> <sub>2</sub> = 0.0742	<i>R</i> <sub>1</sub> = 0.0460 <i>wR</i> <sub>2</sub> = 0.0829

#### 4. Vibrational spectroscopy and solid-state NMR investigations

FTIR spectra were obtained at room temperature by using a Bruker IFS 66v/S spectrometer. The samples were thoroughly mixed with dried KBr (5 mg sample, 500 mg KBr). Raman spectra were excited with a Bruker FRA 106/S module equipped with an Nd-YAG laser ( $\lambda$  = 1064 nm) scanning a range from 100 to 3500 cm<sup>-1</sup>. All sample preparations have been performed in a glove box under dried argon atmosphere.

<sup>11</sup>B, <sup>13</sup>C, <sup>29</sup>Si, and <sup>1</sup>H MAS-NMR spectra were measured with a conventional impulse spectrometer DSX avance (Bruker) operating with a resonance frequency of 500 MHz for <sup>1</sup>H (*B* = 11.3 T). The samples

were filled in zirconia rotors (diameter 4 mm) and mounted in a standard double-resonance MAS probe (Bruker). Most experiments were carried out using an impulse sequence consisting of three back-to-back impulses, which is designed to eliminate unwanted spectral contributions from the probe [8]. For the <sup>1</sup>H, <sup>13</sup>C, and <sup>29</sup>Si spectra the impulse length was adjusted to 3 μs fitting a 90° impulse. <sup>11</sup>B spectra were acquired with a 45° impulse (1.5 μs) adjusted using a solution of boron acid. The recycle delay varied between 10 and 200 s to guarantee total rebuild of magnetization by spin-lattice relaxation. Rotation frequencies between 5 and 12 kHz were chosen. Additionally, cross-polarization <sup>1</sup>H/<sup>13</sup>C double-resonance experiments with contact times between 1 and 20 ms were performed to check whether any detectable hydrogen atoms belong to the same phase as

Table 2  
Atomic coordinates for Ba<sub>7</sub>[SiO<sub>4</sub>][(BO<sub>3</sub>)<sub>3</sub>CN and Sr<sub>7</sub>[SiO<sub>4</sub>][(BO<sub>3</sub>)<sub>3</sub>CN

Atom	Wyckoff-symbol	f. o. f.	<i>x</i>	<i>y</i>	<i>z</i>	<i>U</i> <sub>eq</sub>	<i>U</i> <sub>11</sub>	<i>U</i> <sub>22</sub>	<i>U</i> <sub>33</sub>	<i>U</i> <sub>13</sub>	<i>U</i> <sub>23</sub>	<i>U</i> <sub>12</sub>
Ba(1)	6c	1	0.14442(4)	− <i>x</i>	0.19303(8)	0.0205(2)	0.0182(3)	<i>U</i> <sub>11</sub>	0.0221(4)	0.0007(1)	− <i>U</i> <sub>13</sub>	0.0068(3)
Sr(1)	6c	1	0.14465(8)	− <i>x</i>	0.18595(2)	0.0332(5)	0.0248(5)	<i>U</i> <sub>11</sub>	0.045(1)	−0.0005(4)	− <i>U</i> <sub>13</sub>	0.0089(6)
Ba(2)	6c	1	0.52535(3)	− <i>x</i>	0.3505(1)	0.0118(1)	0.0154(2)	<i>U</i> <sub>11</sub>	0.0092(2)	−0.0002(1)	− <i>U</i> <sub>13</sub>	0.0111(2)
Sr(2)	6c	1	0.52403(6)	− <i>x</i>	0.34576(2)	0.0152(3)	0.0219(4)	<i>U</i> <sub>11</sub>	0.0098(6)	−0.0010(3)	− <i>U</i> <sub>13</sub>	0.0169(5)
Ba(3)	2b	1	1/3	2/3	0.4920(2)	0.0095(2)	0.0094(3)	<i>U</i> <sub>11</sub>	0.0097(4)	0	0	0.0047(1)
Sr(3)	2b	1	1/3	2/3	0.48393(4)	0.0153(5)	0.0147(7)	<i>U</i> <sub>11</sub>	0.017(1)	0	0	0.0074(3)
Si(1)	2b	1	1/3	2/3	0.0832(7)	0.010(1)	0.010(1)	<i>U</i> <sub>11</sub>	0.011(2)	0	0	0.0048(7)
		1	1/3	2/3	0.0774(1)	0.022(2)	0.021(2)	<i>U</i> <sub>11</sub>	0.022(5)	0	0	0.011(1)
O(1)	12d	0.5	0.186(1)	0.563(1)	0.163(1)	0.016(2)						
			0.184(1)	0.547(1)	0.159(2)	0.022(3)						
O(2)	12d	1	0.3964(7)	0.0930(7)	0.0522(8)	0.021(1)	0.019(3)	0.025(3)	0.024(3)	−0.009(3)	−0.002(2)	0.016(2)
			0.3960(8)	0.089(1)	0.0528(1)	0.042(2)	0.024(4)	0.037(8)	0.047(7)	0.022(4)	0.000(4)	0.001(3)
O(3)	6c	1	0.8445(6)	− <i>x</i>	0.308(1)	0.032(2)	0.032(4)	<i>U</i> <sub>11</sub>	0.031(6)	0.007(2)	− <i>U</i> <sub>13</sub>	0.015(5)
			0.8465(9)	− <i>x</i>	0.312(2)	0.073(5)	0.11(1)	<i>U</i> <sub>11</sub>	0.03(1)	−0.016(4)	− <i>U</i> <sub>13</sub>	0.07(1)
O(4)	2b	1	1/3	2/3	0.860(2)	0.012(2)	0.013(4)	<i>U</i> <sub>11</sub>	0.010(5)	0	0	0.007(2)
			1/3	2/3	0.844(3)	0.017(3)	0.019(4)	<i>U</i> <sub>11</sub>	0.013(9)	0	0	0.009(2)
B(1)	6c	1	0.8162(6)	− <i>x</i>	0.136(2)	0.012(2)	0.011(4)	<i>U</i> <sub>11</sub>	0.018(6)	0.002(2)	− <i>U</i> <sub>13</sub>	0.008(4)
			0.8153(7)	− <i>x</i>	0.127(3)	0.014(3)	0.018(5)	<i>U</i> <sub>11</sub>	0.01(1)	−0.004(2)	− <i>U</i> <sub>13</sub>	0.014(6)
N(1)	2a	1	0	0	0	0.08(1)						
		1	0	0	0	0.07(1)						

f. o. f. = fractional occupancy factor and anisotropic displacement parameters (e.s.ds. in parentheses). The anisotropic thermal displacement factor is given as  $\exp[-2\pi^2[(ha^*)^2U_{11} + \dots + 2hka^*b^*U_{12}]]$ . *U*<sub>eq</sub> is defined as one-third of the trace of the orthogonalized *U*<sub>*ij*</sub> tensor.

Table 3  
Interatomic distances/pm and angles/deg (e.s.ds. in parentheses)

Ba1–O1	290(1)	Sr1–O1	261(1)		
Ba1–O2	295.5(7)	Sr1–O2	279(1)		
Ba1–O2	307.6(6)	Sr1–O2	298.6(9)		
Ba1–O3	283(1)	Sr1–O3	261(2)		
Ba1–O3	305.9(7)	Sr1–O3	293(1)		
Ba2–O1	267(1)	Sr2–O1	257(2)	O1–Si1–O1	107.3(5)
Ba2–O1	272(1)	Sr2–O1	258(1)		107.9(7)
Ba2–O2	265.4(6)	Sr2–O2	250.8(8)	O1–Si1–O4	111.5(4)
Ba2–O2	279.9(6)	Sr2–O2	262.1(8)		111.0(7)
Ba2–O3	319.9(8)	Sr2–O3	309(1)		
Ba2–O4	276.66(7)	Sr2–O4	267.6(1)		
Ba3–O1	283(1)	Sr3–O1	270(1)	O2–B–O2	121(1)
Ba3–O2	293.3(7)	Sr3–O2	284.3(9)		129(1)
Ba3–O4	270(2)	Sr3–O4	250(2)	O3–B–O2	119.5(6)
					115.7(8)
Si1–O1	159(1)	Si1–O1	159(1)		
Si1–O4	164(2)	Si1–O4	163(2)		
B1–O2	136.6(8)	B1–O2	132(1)		
B1–O3	138(2)	B1–O3	141(2)		

the carbon atoms. <sup>1</sup>H, <sup>13</sup>C, and <sup>29</sup>Si resonances are reported with respect to TMS and <sup>11</sup>B signals are referenced using the adduct of boron trifluoride and diethyl ether.

Simulations of the spectra were carried out using the program package SIMPSON [9]. For the <sup>13</sup>C and <sup>29</sup>Si MAS-spectra both isotropic and anisotropic parts of the

chemical-shift interaction were considered while for the <sup>11</sup>B MAS-spectra we took into account only second-order quadrupole broadening of the central transition and the isotropic chemical shift. Line-shape changes due to the relative orientation of the tensors of the anisotropic chemical shift and quadrupole interactions were ignored.

## 5. Results and discussion

### 5.1. Structure description

$\text{Ba}_7[\text{SiO}_4][\text{BO}_3]_3\text{CN}$  and  $\text{Sr}_7[\text{SiO}_4][\text{BO}_3]_3\text{CN}$  represent a new structure type. Borosilicates already have been described in the literature [10,11], and silicate cyanides are known as well [12]. However  $\text{Ba}_7[\text{SiO}_4][\text{BO}_3]_3\text{CN}$  and  $\text{Sr}_7[\text{SiO}_4][\text{BO}_3]_3\text{CN}$  are the first examples which contain all the three discrete anions  $[\text{SiO}_4]^{4-}$ ,  $[\text{BO}_3]^{3-}$ , and  $\text{CN}^-$  in one ionic compound (Fig. 1). The disordered cyanide anions are octahedrally coordinated by  $\text{Ba}^{2+}$  or  $\text{Sr}^{2+}$ , respectively. The cations form regular face sharing octahedra around the  $\text{CN}^-$  building chains along [001]. These chains are surrounded by three  $[\text{BO}_3]^{3-}$  units per octahedron and they are orientated in a way that two O atoms of each  $[\text{BO}_3]^{3-}$  ion are positioned over two faces of neighboring octahedra (Figs. 5 and 6).

The  $[\text{SiO}_4]^{4-}$  ions are coordinated by 11 cations. Four of them form a regular tetrahedron around the  $[\text{SiO}_4]^{4-}$  units (Fig. 2). The coordination numbers of the cations vary between 9 and 11, which is quite ordinary for alkaline earth cations (Fig. 3). The surrounding of the  $[\text{BO}_3]^{3-}$  units is a three-capped trigonal prism of cations, in which each O atom is located in the center of a quadratic pyramid (Fig. 4).

The  $[\text{SiO}_4]^{4-}$  ions are tetrahedrally coordinated by four cations. The coordination numbers of the cations vary between 9 and 11 anions, which is quite ordinary for alkaline earth cations (Fig. 2).

Since the radius of  $\text{Cl}^-$  and  $\text{CN}^-$  is similar it could have been possible that this site was occupied with  $\text{Cl}^-$  ions instead of  $\text{CN}^-$ . A chemical analysis of the compounds unequivocally proved the presence of cyanide and excluded chloride, however we additionally investigated the compounds by vibrational spectroscopy and MAS-NMR.

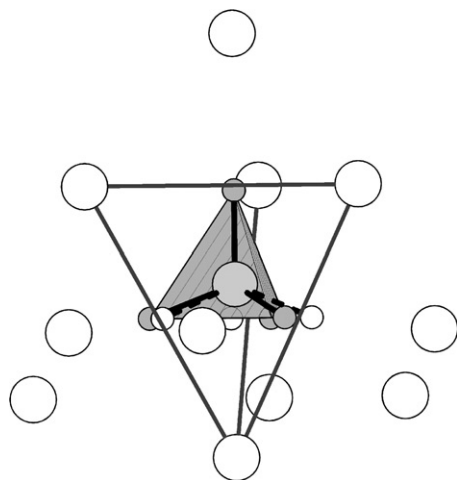


Fig. 2. Coordination of the  $[\text{SiO}_4]^{4-}$  ion, for color codes see Fig. 1.

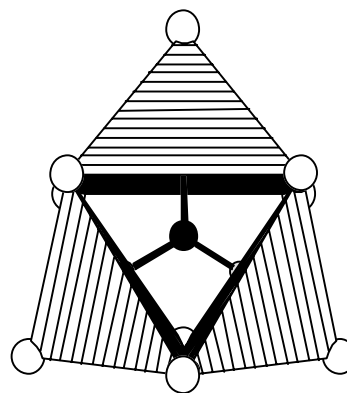


Fig. 3. Coordination of the  $[\text{BO}_3]^{3-}$  unit.

### 5.2. Spectroscopy

To verify the existence of isolated  $\text{CN}^-$ ,  $[\text{BO}_3]^{3-}$ , and  $[\text{SiO}_4]^{4-}$  units Raman and IR spectra as well as  $^{11}\text{B}$ ,  $^{13}\text{C}$ , and  $^{29}\text{Si}$  MAS-NMR investigations were performed for  $\text{Ba}_7[\text{SiO}_4][\text{BO}_3]_3\text{CN}$  at room temperature (see Figs. 7 and 8).

First we checked for absence of hydrogen atoms by collecting a proton NMR spectrum. The  $^1\text{H}$  MAS spectrum shows only very weak signal intensities indicating that these resonances are due to small impurities or due to water absorbed on the surface of the sample. To ensure that the hydrogen atoms are not part of the identified silicate borate cyanides we used a cross-polarization (CP) sequence to excite  $^{13}\text{C}$  nuclei via  $^1\text{H}$ . If both types of nuclei belong to the same phase polarization transfer from hydrogen to carbon should be possible. We used contact times ranging from 1 to 20 ms. However, we were not able to excite carbon nuclei with this technique, thus excluding protons in the main phase.

The Raman and IR spectra (Fig. 7) show several strong signals in the range of  $2000\text{--}2200\text{ cm}^{-1}$ , which are typical for  $\text{CN}^-$  ions [13,14]. Furthermore, the  $^{13}\text{C}$  spectrum exhibits two signals, one sharp resonance at  $180.0(1)\text{ ppm}$  (FWHM = 1 ppm) and a broad resonance at about  $178\text{ ppm}$  (FWHM  $\approx 6\text{--}7\text{ ppm}$ ). The latter is probably due to an amorphous impurity of roughly 30%. According to the reaction conditions only graphite or cyanides as impurities seem reasonable. However, the resonance of amorphous graphite is found in the range  $110\text{--}120\text{ ppm}$  in the literature [15]. Furthermore, due to the large anisotropic magnetic susceptibility we would expect it to be extremely broad (FWHM  $\approx 200\text{ ppm}$ ) [16,17]. Since neither the position nor the width of the highfield shifted signal ( $178\text{ ppm}$ ) fits to the above-mentioned conditions, we excluded graphitic impurities. In the literature not many reference values for isolated cyanide ions in inorganic salts were reported. Therefore,

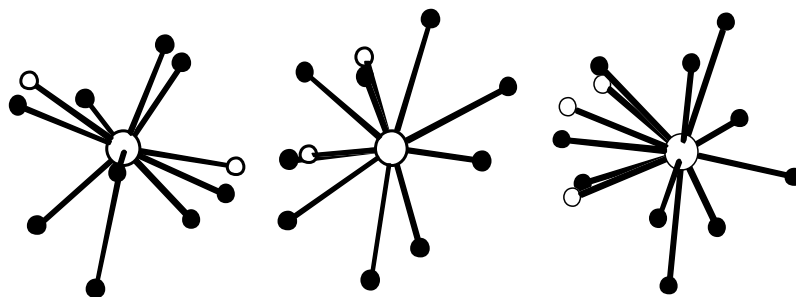


Fig. 4. Coordination of the alkaline earth ions M1, M2, M3 by oxygen from left to right. Split position of O1 depicted as small white circles.

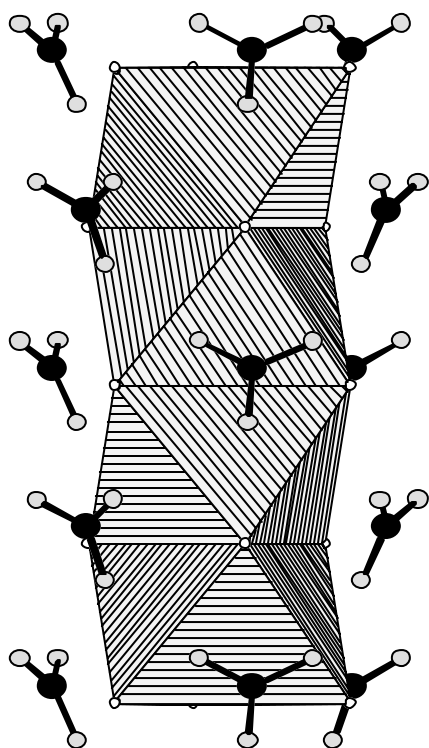


Fig. 5.  $\text{Ba}^{2+}/\text{Sr}^{2+}$  octahedra around the disordered  $\text{CN}^-$  ions with the surrounding  $[\text{BO}_3]^{3-}$  unities, view along  $[-\frac{1}{2}0]$ .

we recorded the  $^{13}\text{C}$  NMR spectrum of pure KCN (Merck, purity 97%) as determined by X-ray diffraction, which shows one sharp  $^{13}\text{C}$  resonance at 169.3 ppm. The cyanide ions in both substances  $\text{Ba}_7[\text{SiO}_4][\text{BO}_3]_3\text{CN}$  and KCN are octahedrally coordinated by cations and are thus comparable. However, the doubled positive charge of the cations in  $\text{Ba}_7[\text{SiO}_4][\text{BO}_3]_3\text{CN}$  as compared to KCN leads to a significant reduction of the charge density at the carbon atom, resulting in a shift of 10.7 ppm of the  $^{13}\text{C}$  signal to higher frequencies. This trend similarly is observed for  $\text{CN}^-$  ions dissolved in methanol [18]. The solvation with methanol increases the charge density at the  $\text{CN}^-$  group leading to a highfield shift to 161.2 ppm. Thus both resonances can be assigned to cyanide ions.

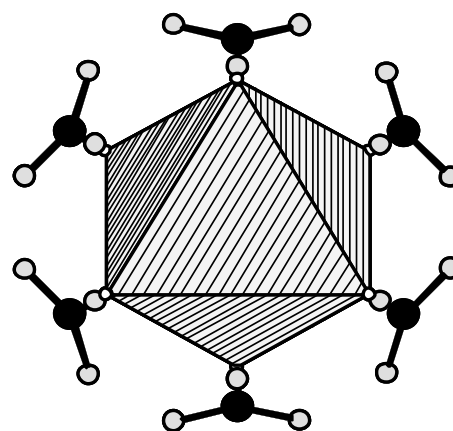


Fig. 6.  $\text{Ba}^{2+}$  octahedra with surrounding  $[\text{BO}_3]^{3-}$  ions, view along [001].

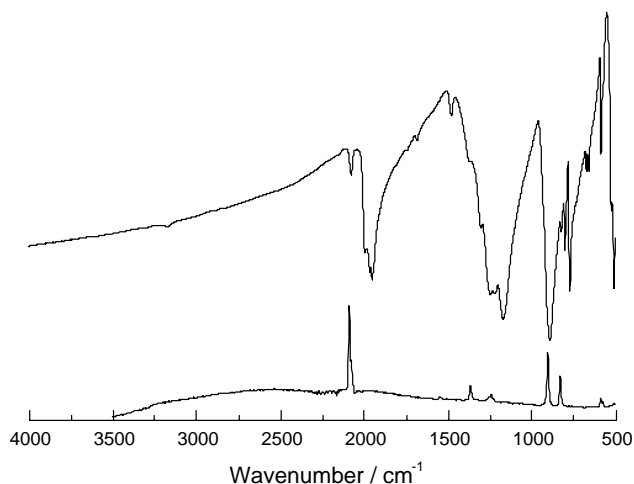


Fig. 7. IR (top) and Raman (bottom) spectra of  $\text{Ba}_7[\text{SiO}_4][\text{BO}_3]_3\text{CN}$ .

Both vibrational and NMR spectroscopy prove the existence of isolated cyanide anions as proposed from our single-crystal X-ray diffraction data.

Between 1350 and  $500\text{ cm}^{-1}$  we observed several sharp peaks in the Raman spectrum which can be assigned to either isolated borate or silicate groups [14,19]. Only the

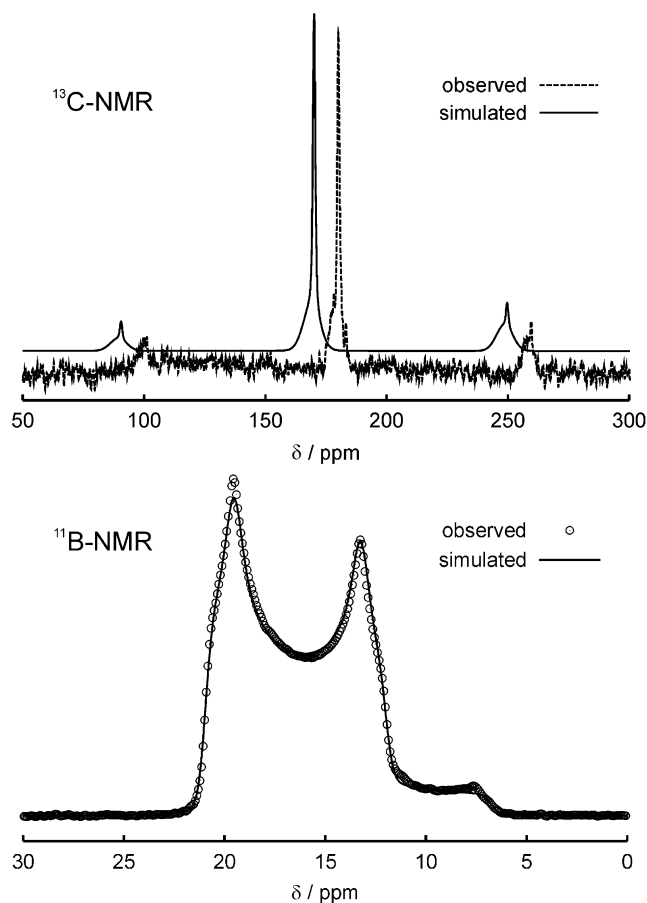


Fig. 8. Profile fits of an  $^{13}\text{C}$ -MAS-NMR and an  $^{11}\text{B}$ -MAS-NMR spectrum measured at room temperature with rotation frequencies of 10 and 12 kHz, respectively. The observed MAS spectrum for  $^{13}\text{C}$  is depicted with dashed lines. For an easier comparison of the observed and simulated data (solid lines) the simulation was shifted 10 ppm to the left and upwards. In the case of the  $^{11}\text{B}$  NMR spectrum the open circles represent the measurement and the solid line the simulation. Details of the refinement results are given in the text.

resonance at  $1364\text{ cm}^{-1}$  unambiguously belongs to  $[\text{BO}_3]^{3-}$ . Due to the broad and heavy overlapping of signals in the same region no reliable assignment of the bands in the IR spectrum was possible [20].

The  $^{29}\text{Si}$  MAS-NMR spectrum consists of two sharp resonances (FWHM = 0.7 ppm) at  $-69.4(1)$  ppm (strong) and  $-70.2(1)$  ppm (weak). The intensity ratio is about 5:1 and the weak signal at  $-70.2$  ppm can probably be assigned to the same X-ray amorphous impurity as discussed for the  $^{13}\text{C}$  spectrum. The value of  $-70$  ppm for  $^{29}\text{Si}$  resonances is typical for  $\text{Q}^0$  units [21] and verifies the existence of isolated  $[\text{SiO}_4]^{4-}$  ions in the structure of  $\text{Ba}_7[\text{SiO}_4][\text{BO}_3]_3\text{CN}$ .

Finally an  $^{11}\text{B}$  MAS-NMR spectrum was measured with a rotation frequency of 12 kHz. For our analysis we focussed on the region where the central transition is observed neglecting the very broad satellites. The central band consists of one broad, structured resonance in the

range  $5\text{ ppm} \leq \delta \leq 25\text{ ppm}$  (see Fig. 8), which could be simulated in excellent agreement assuming only one crystallographic boron site and taking into account only second order quadrupole broadening as well as the isotropic chemical shift. Line broadening effects due to finite spin–spin relaxation were considered by convoluting the simulated spectrum with a Gaussian function. The resulting quadrupole coupling constant  $\delta_Q = 2.51\text{ MHz}$  and isotropic chemical shift  $\sigma_{\text{iso}} = 22.2\text{ ppm}$  suit well to values reported in the literature [22] for  $\text{T}^0$  or  $\text{T}^1$  coordinated borate groups. However, for  $\text{T}^1$  units the quadrupole interaction is expected to be highly asymmetric ( $\eta \approx 0.5$ ), whereas in the case of isolated borate groups ( $\text{T}^0$ ) it should exhibit almost axial symmetry ( $\eta \leq 0.1$ ). The observed asymmetry parameter in the case of  $\text{Ba}_7[\text{SiO}_4][\text{BO}_3]_3\text{CN}$  is  $\eta = 0.160$  which is close to axial symmetry. Taking into account the site symmetry  $m$  of the borate group a non-axial symmetric quadrupole coupling tensor is in full agreement with the single-crystal data, where two different B–O distances ( $2 \times \text{B1–O2}$  137(1) pm,  $1 \times \text{B1–O3}$  138(2) pm) were found. Thus the line-shape analysis of the  $^{11}\text{B}$ -MAS spectrum confirms the existence of isolated three-fold coordinated borate groups as proposed by the X-ray single-crystal diffraction measurements.

Supplementary material concerning the single-crystal structure analyses have been sent to the Fachinformationszentrum Karlsruhe, Abt. PROKA, D-76344 Eggenstein-Leopoldshafen, Germany, and can be obtained by contacting the FIZ (quoting the article details and the corresponding number CSD-412891 ( $\text{Sr}_7[\text{SiO}_4][\text{BO}_3]_3\text{CN}$ ) and CSD-412890 ( $\text{Ba}_7[\text{SiO}_4][\text{BO}_3]_3\text{CN}$ )).

## Acknowledgments

Financial support by the Fonds der Chemischen Industrie, Germany, the Bundesministerium für Bildung und Forschung (bmbf) and especially by the Deutsche Forschungsgemeinschaft (Gottfried-Wilhelm-Leibniz-Programm) is gratefully acknowledged. The authors thank Dr. P. Mayer and Dr. H.A. Höpfe for recording the single-crystal diffraction data.

## References

- [1] W. Schnick, *Int. J. Inorg. Mater.* 3 (2001) 1267.
- [2] [a] M. Orth, W. Schnick, *Z. Anorg. Allg. Chem.* 625 (1999) 551;  
[b] M. Orth, R.-D. Hoffmann, R. Pöttgen, W. Schnick, *Chem. Eur. J.* 7 (2001) 2791.
- [3] S. Schmid, W. Schnick, *Z. Anorg. Allg. Chem.* 628 (2002) 1192.
- [4] W. Schnick, H. Huppertz, R. Lauterbach, *J. Mater. Chem.* 9 (1999) 289.

- [5] G. Brauer, Handbuch der Präparativen Anorganischen Chemie, 3rd Edition, Ferdinand Enke Verlag, Stuttgart, 1978.
- [6] G.M. Sheldrick, SHELX-97, University of Göttingen, 1997.
- [7] L.J. Farrugia, J. Appl. Crystallogr. 32 (1999) 837.
- [8] S. Zhang, X. Wu, M. Mehring, Chem. Phys. Lett. 173 (1990) 481.
- [9] M. Bak, J.T. Rasmussen, N.C. Nielsen, J. Magn. Reson. 147 (2000) 296.
- [10] D.R. Peacor, R.C. Rouse, E.S. Grew, Am. Miner. 84 (1999) 1152.
- [11] Y. Hiroi, E.S. Grew, Y. Motoyoshi, D.R. Peacor, R.C. Rouse, S. Matsubara, K. Yokoyama, R. Miyawaki, J.J. McGee, S.-Ch. Su, T. Hokada, N. Furukawa, H. Shibasaki, Am. Miner. 87 (2002) 160.
- [12] F. Hund, Z. Anorg. Allg. Chem. 511 (1984) 225.
- [13] D. Durand, L.C. Scavarda do Carmo, F. Lüty, Phys. Rev. B 19 (1989) 6096.
- [14] J. Weidlein, U. Müller, K. Dehnicke, Schwingungsfrequenzen I, Georg Thieme Verlag Stuttgart, New York, 1981.
- [15] J.C.C. Freitas, F.G. Emmerich, G.R.C. Cernicchiaro, L.C. Sampaio, T.J. Bonagamba, Solid State Nucl. Magn. Reson. 20 (2001) 61.
- [16] D.L. VanderHart, W.L. Earl, A.N. Garroway, J. Magn. Reson. 44 (1981) 361.
- [17] M. Alla, E. Lippmaa, Chem. Phys. Lett. 87 (1982) 30.
- [18] A. Kornath, O. Blecher, Z. Naturforsch. 54b (1999) 372.
- [19] Y. Shi, J. Liang, H. Zhang, J. Yang, W. Zhuang, G. Rao, J. Solid State Chem. 129 (1997) 45.
- [20] J. Weiler, Nature 130 (1932) 893.
- [21] N. Janes, E. Oldfield, J. Am. Chem. Soc. 107 (1985) 6769.
- [22] S. Kroeker, J.F. Stebbins, Inorg. Chem. 40 (2001) 6239.
- [23] XRED, Revision 1.19, Stoe & Cie GmbH, Darmstadt, 1999.